


Three-stage thermalization of a quasi-integrable system

Leonardo Biagetti, Guillaume Cecile, and Jacopo De Nardis

*Laboratoire de Physique Théorique et Modélisation, CNRS UMR 8089, CY Cergy Paris Université,
95302 Cergy-Pontoise Cedex, France*

 (Received 4 August 2023; revised 17 January 2024; accepted 31 January 2024; published 22 April 2024)

We consider a system of classical hard rods or billiard balls in one dimension, initially prepared in a Bragg-pulse state at a given temperature and subjected to external periodic fields. We show that at late times the system thermalizes in the thermodynamic limit via a three-stages process characterized by: an early phase where the dynamics is well described by Euler hydrodynamics, a subsequent phase where a (weak) turbulent phase is observed and where hydrodynamic gradient expansion can be broken, and a final one where the gas thermalizes according to viscous hydrodynamics. As the hard rod gas shares the same large-scale hydrodynamics as other quantum and classical integrable systems, we expect these features to universally characterize all many-body integrable systems in generic external potentials.

DOI: [10.1103/PhysRevResearch.6.023083](https://doi.org/10.1103/PhysRevResearch.6.023083)

I. INTRODUCTION

Interacting many-particle systems are notorious for bringing up new emergent physical behaviors at large scales that would be impossible to observe at the level of their elementary constituents. Understanding and classifying the emergent laws of nonequilibrium many-body dynamics is, therefore, one of the main focuses of present-day physics. In the past years, a lot of effort has been put into understanding the equilibration and thermalization mechanism of isolated many-body interacting systems, at theoretical [1–5] and experimental level [6–13]. Indeed, while the postulates of statistical physics indicate that eventually, the system thermalizes, or at least it explores equally all the phase space at its disposal, much less is known about the approach to equilibrium, especially with regard to quantum systems [2,14–16]. Violation of canonical thermalization on the other hand, can be observed in the presence of extra symmetries, for example, local symmetries, or extensive ones, as it is the case for localized or integrable systems [15–18]. There, despite conserved quantities are typically broken at large times in real settings, the dynamics of quasi-integrable systems is of extreme interest, as numerous experimental settings are much better described by integrable systems than fully nonintegrable ones [6–12]. Global integrability is typically broken by other Hamiltonian terms, such as the harmonic trap in a cold atomic setting, or an inhomogeneous magnetic field. As a full quantum problem is hard to numerically simulate for a long time, it is advisable to introduce toy models that are expected to display the same physics as the real quantum ones.

One of them is the *hard rod gas*, namely billiard balls with a fixed diameter d in one dimension that scatters elastically at

each collision. The model is clearly integrable [19–21] as all the initial momenta of the rods are preserved by dynamics, and it has been shown [19,22] to be described at large scale by the same hydrodynamics characterizing generic integrable systems [23,24], i.e. generalized hydrodynamics (GHD) [25,26] (see also various applications to cold atomic as well as spin and fermionic systems [24,27–38]). Moreover, the dynamics with integrability breaking terms in the hard rod gas has been the subject of numerous studies recently [39] as indeed it is expected to display many similarities with the one observable in quantum gases.

In this letter, we study a model of hard rods in the presence of external inhomogeneous potentials. We consider both a trapping potential $V(x)$ and a spacial dependent mass $m(x)$. While the latter may sound artificial, it actually mimics the dynamics of quasiparticles in spin chains under inhomogeneous magnetic fields (as the magnetic field gives an effective mass to the magnonic degrees of freedom, see for example, Refs. [40,41]). We here show that the system thermalizes as long as external fields are finite and inhomogeneous by means of an effective *viscous hydrodynamics*. We observe that the thermalization dynamics can be split into three main phases in time: (I) an *Euler phase* where the dynamics almost follow the one of the Euler GHD equations, (II) a *turbulent phase*, in close agreement with two-dimensional wave turbulence [42] phenomenology, where the state of the system deviates from the viscous hydrodynamics prediction due to the proliferation of hydrodynamic modes with high momenta. And finally, (III) a *diffusively thermalizing phase* where the thermal state is approached exponentially with a time scale set by the diffusion constant of the final thermal state, fixed by the viscous GHD. While in phase I and III, viscous GHD equation correctly capture *quantitatively* the dynamics of the gas, it can fail to give correct predictions in phase II, due to a turbulence-induced *gradient catastrophe*, induced by the creation of fine structures in the fluid density by the chaotic Euler evolution. However, if the initial momentum distribution is smooth, as in the case of initial high temperature, the effect of such a

Published by the American Physical Society under the terms of the [Creative Commons Attribution 4.0 International](https://creativecommons.org/licenses/by/4.0/) license. Further distribution of this work must maintain attribution to the author(s) and the published article's title, journal citation, and DOI.

turbulent phase is reduced and viscous GHD captures the whole thermalization dynamics.

The hard rod gas. We consider a system of N billiard balls of diameter d on a circle of length L with Hamiltonian given by

$$H = \sum_{i=1}^N \left[\frac{\theta_i^2}{2m(x_i)} + V(x_i) \right] + \sum_{i<j} U(x_i - x_j), \quad (1)$$

where θ_i^2 is the momentum of each particle with its center positioned in x_i , and where the interaction potential is the one describing hard spheres (Tonks gas), $U(x) = \infty$ for $|x| \leq d$ and $U(x) = 0$ for $|x| > d$. In this letter we consider time-independent periodically varying external potentials, with a wavelength ℓ , namely, we consider

$$m(x) = m \left(1 + \frac{m_0}{m} \cos(2\pi x/\ell) \right)^{-1};$$

$$V(x) = V_0 \cos(2\pi x/\ell), \quad (2)$$

and we set $m = 1$ generically. The Hamiltonian (D1) with $V_0 = m_0 = 0$ is integrable and is well studied in the literature [43–47]. As scatterings are all elastic, the initial values of the momenta θ_i of the rods are conserved, giving N integrals of motions. A generic stationary state of the integrable model, with zero external fields, is given by a so-called generalized Gibbs ensemble (GGE) [18], namely a thermodynamic state where entropy is maximized given a distribution of momenta $\rho(\theta)$. One can simply use the mapping from free particles to hard-core ones to initialize the system in such a state, in particular, the spatial distribution of the particles is taken to be a Poisson point process [20,48]. Such an initial state, when averaged over different realizations, has all the correct statistical properties of a GGE, i.e., the average number of particles in an interval Λ is $\langle dN(\theta, \Lambda) \rangle = \rho(\theta)\Lambda$ and their fluctuations are given by the correct susceptibility matrix (for its explicit definition see, for example, [22]) $C(\theta, \theta')\Lambda = \langle dN(\theta, \Lambda)dN(\theta', \Lambda) \rangle^c$. In this work, simulations are performed always on a ring of length $L = 10^3$, with $N = L/2$ particles and by averaging over 3×10^3 initial configurations.

II. VISCOUS GHD

The HR gas, despite being a purely classical model, shares exactly the same large-scale hydrodynamics with other quantum and classical integrable models, i.e., the GHD, where the distribution of the rods momenta $\rho(\theta, x, t)$ at position x and time t is taken as the effective hydrodynamic fluid density. In the purely integrable case, there is no flow in the θ space, as all the momenta are conserved. However, in the presence of external forces, the flow in θ space gets activated. Indeed, switching on external potentials generically leads to integrability breaking. The momenta are not conserved any more and the resulting equations of motions for the rods, whenever the rod i is not in contact with any of the other rods, result in $\dot{x}_i(t) = \frac{\theta_i(t)}{m(x_i)}$ and $\dot{\theta}_i(t) = a_i(t)$, with acceleration $a_i(t) = f_1(x_i) + \theta_i^2 f_2(x_i)/2$, where we introduced the forces $f_1(x) = -\partial_x V$ and $f_2(x) = -\partial_x(m(x)^{-1})$. Including exact viscous dissipative terms, the relevant hydrodynamic equation takes the form of a two-dimensional fluid in the

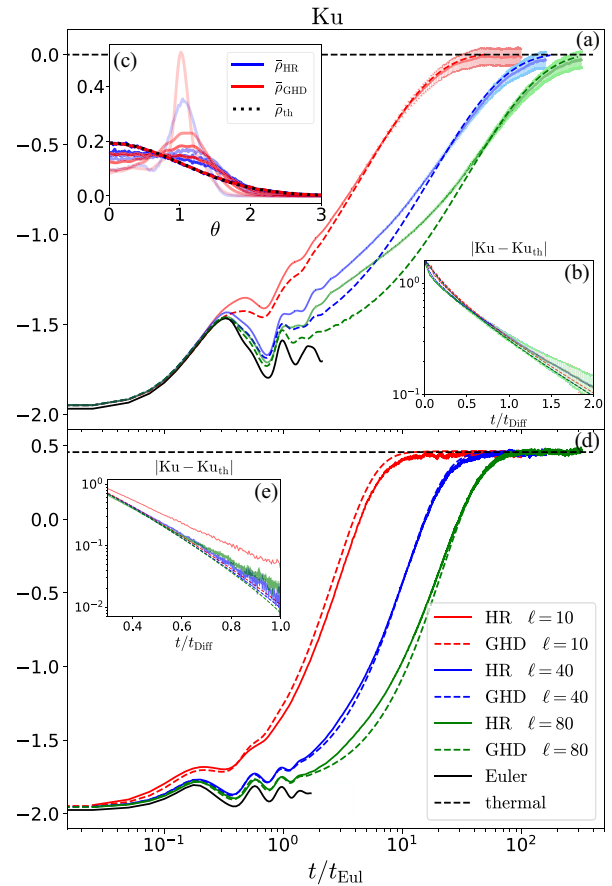


FIG. 1. Comparison of kurtosis of the spatially integrated $\rho(\theta, x, t)$ of the exact hard rod (HR) gas dynamics with $d = 1$, and its diffusive GHD prediction, Eq. (3) (the inviscid Euler hydrodynamics at short times is also reported in black), with (a), (b), (c) $V_0 = 0.5, m_0 = 0$ and (d), (e) $V_0 = 0, m_0 = 0.5$, initialized in a Bragg pulse state with low temperature $T_0 = 0.01$. (a), (d) show time evolution as a function of t/t_{Eul} and the insets b,e the approach to thermalization as a function of t/t_{Diff} . (c) shows the spatially integrated $\rho(\theta, x, t)$ for both GHD prediction and exact hard rod gas dynamics for $t/t_{\text{Eul}} = 0.5, 5, 10, 20, 160$ (increasing from light to dark) and the expected spatially integrated thermal distribution.

effective space (θ, x) , with associated gradient $\nabla = (\partial_x, \partial_\theta)$, flow vector $\mathbf{J}_{[\rho]}^{\text{eff}} = (v_{[\rho]}^{\text{eff}}, a_{[\rho]}^{\text{eff}})$ and diffusion matrix $\mathfrak{D}_{[\rho]}$ [whose definition is given in Eq. (5)], reading as

$$\partial_t \rho + \nabla \cdot (\mathbf{J}_{[\rho]}^{\text{eff}} \rho) = \frac{1}{2} \nabla \cdot (\mathfrak{D}_{[\rho]} \nabla \rho). \quad (3)$$

This equation is conjectured to describe generic integrable systems under external fields, and it was first derived in full generality in Ref. [49]. In Appendix D is given an intuitive derivation in the case of the hard rod gas only based on the kinetic picture, in the same spirit as in Refs. [50,51]. In order to define the flow vector and the diffusive matrix, it is useful to move from the elementary rods to the quasiparticle tracers. The tracers are defined as labels associated with the rods. During a scattering, the two rods exchange the tracer label. Such tracers, therefore, move throughout the system, experiencing jumps in space and momenta at each scattering with other particles. Therefore, at the mesoscopic scale, the phase space dynamics depends on the local density $\rho(\theta, x)$

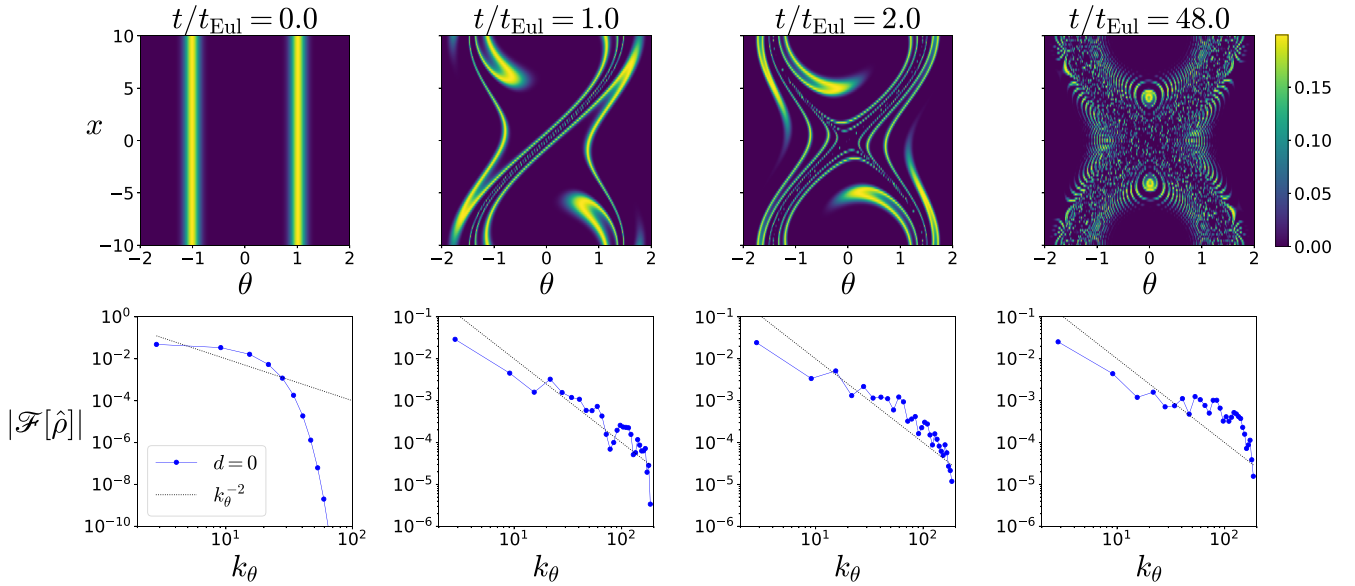


FIG. 2. Euler scale GHD evolution for $d = 0$ with $m_0(x) = 0$, $V_0 = 0.5$ and $\ell = 5$, initialized in a Bragg pulse state with width $T_0 = 0.01$: (top) Plot of the spatially integrated density as function of momentum θ and position x . (bottom) Log-Log plot of the absolute value of the Fourier transform in θ of the spatially integrated density as a function of Fourier vector k_θ . At $t = 0$ the decay is exponential while within the turbulent phase $t/\ell \gtrsim 1$ we observe the (fitted) decay $k_\theta^{-\alpha}$ with $\alpha \sim 2$. We stress that, in the noninteracting particles limit $d = 0$, the Euler scale GHD is exact at all times.

and is described by the flow vector

$$\mathbf{J}_{[\rho]}^{\text{eff}} = \begin{pmatrix} v_{[\rho]}^{\text{eff}} = (\theta - \overline{\rho\theta d}) / (m(x)(1 - \overline{\rho d})) \\ a_{[\rho]}^{\text{eff}} = f_1 + f_2(\theta^2/2 - \overline{\rho\theta^2 d/2}) / (1 - \overline{\rho d}) \end{pmatrix}, \quad (4)$$

where overlined quantities denote integral over momenta $\bar{f} = \int d\theta f(\theta)$. Since the hydrodynamic flow (4) depends nontrivially on the local particle density $\rho(\theta, x)$, it is subjected to a diffusive broadening due to its local finite thermodynamic fluctuations defined by the susceptibility matrix $C(\theta, \theta')$. Notice that in nonintegrable systems such quadratic fluctuations of convective currents give generically only a lower bound to the diffusion constants [52], while in integrable ones they fully saturate them [53]. Here we show that the latter remains true also in quasi-integrable systems.

The diffusion coefficients $\mathfrak{D}_{[\rho]}$ are then defined as generators of reversible Markov jump processes induced by such density fluctuations [19,23] and are equal to

$$\mathfrak{D}_{[\rho]} = \delta_{\theta, \theta'} \int_{\mathbb{R}} d\theta'' \rho(\theta'', x) \mathbf{g}(\theta, \theta'') - \rho(\theta', x) \mathbf{g}(\theta, \theta'), \quad (5)$$

where $\delta_{\theta, \theta'}$ is the Dirac delta in the momenta space and the kernel matrix \mathbf{g} is defined by

$$\frac{\mathbf{g}}{d^2} = \begin{pmatrix} |v_{[\rho]}^{\text{eff}}(\theta) - v_{[\rho]}^{\text{eff}}(\theta')| & \xi_{\theta, \theta'} (a_{[\rho]}^{\text{eff}}(\theta) - a_{[\rho]}^{\text{eff}}(\theta')) \\ \xi_{\theta, \theta'} (a_{[\rho]}^{\text{eff}}(\theta) - a_{[\rho]}^{\text{eff}}(\theta')) & \frac{(a_{[\rho]}^{\text{eff}}(\theta) - a_{[\rho]}^{\text{eff}}(\theta'))^2}{|v_{[\rho]}^{\text{eff}}(\theta) - v_{[\rho]}^{\text{eff}}(\theta')|} \end{pmatrix}, \quad (6)$$

with $\xi_{\theta, \theta'} \equiv \text{sgn}(v_{[\rho]}^{\text{eff}}(\theta) - v_{[\rho]}^{\text{eff}}(\theta'))$ (for a full derivation from kinetic theory see Appendix D). While the left-hand side of Eq. (3), which corresponds to the Euler GHD equation, has numerous integrals of motion [54,55] and does not thermalize, one can show (see Appendix C) that the viscous terms on the right-hand side break most of the conservation laws,

and the fixed point of Eq. (3) is a thermal local density approximation state, (as discussed also in Refs. [49,56]) determined only by the inverse temperature β and chemical potential μ , fixed by the only conserved quantities: the integrated density $N_0 = \int dx \int d\theta \rho(\theta, x, 0)$ and energy $E_0 = \int dx \int d\theta \rho(\theta, x, 0)(\theta^2/(2m(x)) + V(x))$. In terms of these parameters, the thermal distribution reads

$$\rho_{\text{th}}(\theta; x) \sim e^{-\beta(m(x)\theta^2/2 + V(x) - \mu)}. \quad (7)$$

We here will consider the integrated distribution in space $\hat{\rho}(\theta, t) = \int dx \rho(\theta, x, t)$ and show that at late times thermalization is achieved $\hat{\rho}(\theta, t) \rightarrow \hat{\rho}_{\text{th}}(\theta)$ under the effect of the external forces and internal viscosities, by means of the mechanism we describe below.

III. THE THREE-STAGE THERMALIZATION

We now focus on a concrete example of dynamics from an initial state. We mimic the state created by a strong Bragg pulse in cold atomic gas, as done for example in [6,13]. In the context of the hard rods, we prepare a spatially homogenous gas with a distribution of momenta given by two Gaussian peaks with a given initial temperature T_0

$$\rho(\theta, x, t = 0) \sim e^{-\frac{(\theta - \theta_{\text{Bragg}})^2}{2T_0}} + e^{-\frac{(\theta + \theta_{\text{Bragg}})^2}{2T_0}}, \quad (8)$$

with normalization fixed by density $\bar{\rho} = 1/2$ and with $\theta_{\text{Bragg}} = 1$ here for convenience. We then let the system evolve under an external field, either with V_0 or m_0 finite. We solve the GHD Eq. (3) by means of a combined fourth-order Runge-Kutta method as defined in Ref. [57] and an implicit midpoint method and by rescaling space x and time t by ℓ , which allows solving it in $x \in [0, 1]$, by adding a factor $1/\ell$ in front of the diffusive terms. We compare the GHD prediction with exact numerical simulations of hard rods, see Appendix A for

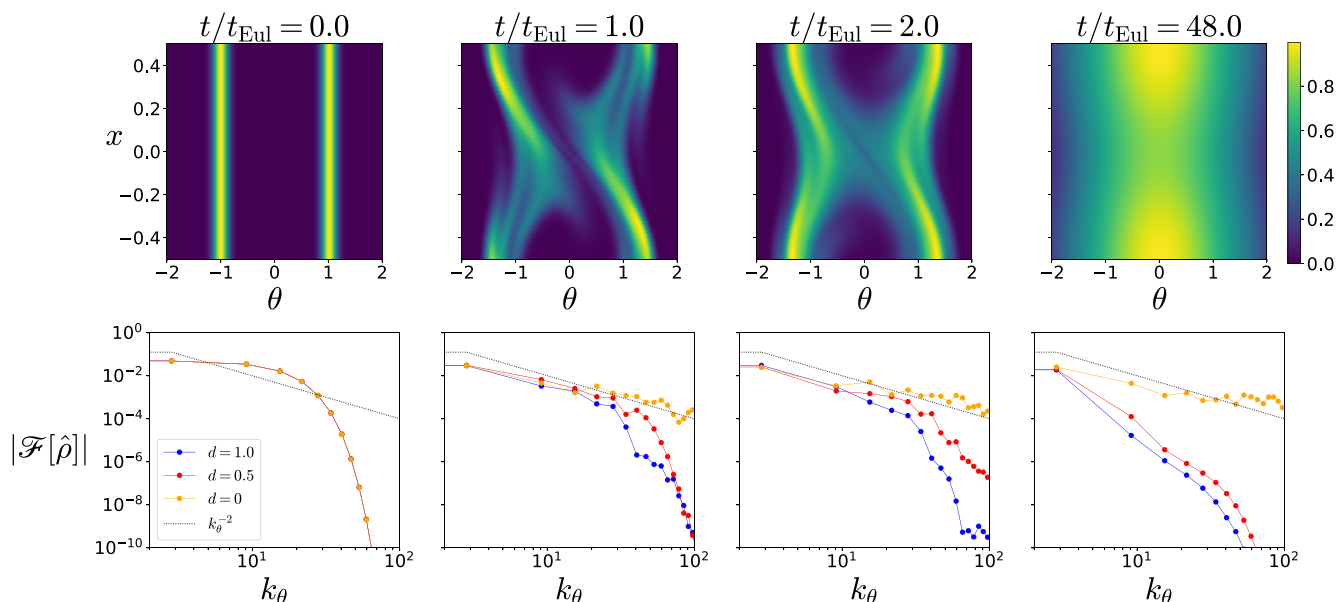


FIG. 3. GHD evolution, Eq. (3), with $m_0 = 0$ and $V_0 = 0.5$ and $\ell = 80$, initialized in a Bragg pulse state with $T_0 = 0.01$: (top) density plot of the density $\rho(\theta, x, t)$ as function of momentum θ and position x at different times, for rods with length $d = 1$. (bottom) Log-Log plot of the absolute value of the Fourier transform in θ of the spatially integrated density as a function of Fourier vector k_θ and three different values of the rods' length d . At time $t = 0$ the decay is exponential while within the turbulent phase $t_{\text{Eul}} \lesssim t \lesssim t_{\text{Diff}}$, we observe the decay as $k_\theta^{-\alpha}$ with $\alpha \sim 2$ in a range of $k_\theta \lesssim 1/\Lambda_{\text{sink}}$ with $\Lambda_{\text{sink}} \sim \bar{\rho}d^2$. The plot for the mass field $m_0 = 0.5$ and $V_0 = 0$, as well as with the exact hard rods simulations, is in Appendix E.

details on the algorithm. We focus on the integrated density $\hat{\rho}(\theta)$ (which can be obtained by a trap-release protocol in a cold atomic setting [12,58]) and in particular on its kurtosis $\text{Ku}(t) = \overline{\theta^4}/(\overline{\theta^2})^2 - 3$ with the overline average taken with $\hat{\rho}(\theta, t)$ as a measure, see Fig. 1. When $m_0 = 0$, thermalisation is manifested by $\text{Ku}(t) \rightarrow 0$ at large times, signaling that the integrated distribution converges to its thermal value (7). However, when $m_0 \neq 0$ the integrated thermal distribution is not a Gaussian, as can be seen from expression (7) and a different value of nonzero kurtosis is therefore expected at large times. For values of ℓ relatively large to ensure the validity of the fluid cell approximation, at times $t \lesssim t_{\text{Eul}} \equiv \ell m/\theta_{\text{Bragg}}$ we always observe agreement between numerical hard rods simulations and viscous GHD, where the latter can also be simplified to its Euler formulation with no dramatic change of behavior, see Fig. 1 where the Euler GHD prediction is reported (up to the time after which the numerical simulation becomes unstable). We denote this phase as the Euler phase, where the dynamics is purely given by an adiabatic Euler flow. As soon as time becomes comparable with $\sim t_{\text{Eul}}$ something dramatic happens: when the gas initial temperature is small $T_0/(\theta_{\text{Bragg}}^2) \ll 1$, the exact numerical simulations and the hydrodynamic predictions do not agree any more, even for large ℓ (actually larger is ℓ , stronger are the deviations from hydrodynamics). We denote this phase as the *turbulent phase*. This phase is characterized by a proliferation of discontinuities in the derivative of the momentum distribution $\rho(\theta, x, t)$, causing the hydrodynamic gradient expansion to break down (gradient catastrophe), *whenever the gas is interacting* (a similar mechanism for free fermion gases was discussed in Ref. [59]). In order to quantify such a discontinuous behavior, we plot the absolute value of the

Fourier transform in θ of the integrated momenta distribution $|\mathfrak{F}[\hat{\rho}](k_\theta)| = |\int d\theta e^{ik_\theta\theta} \hat{\rho}(\theta, t)|/2\pi$, see Figs. 2 and 3. The latter decays exponentially in k_θ at short times (being the Fourier transform of two Gaussian peaks) to then develop a power law decay as k_θ^{-2} , compatible with the presence of cusps. In the free particle case $d = 0$, the same proliferation of discontinuities in the single particle density $\hat{\rho}(\theta)$ occurs as shown in Fig. 2, but being Euler hydrodynamics the exact description of the system, with no higher derivative terms, no breaking of hydrodynamics expansion occurs. This clarifies that such proliferation of discontinuities is purely generated by the chaotic Euler dynamics, but it is only in the interacting case $d > 0$ where this causes the breaking of hydrodynamics, due to the breaking of the hydrodynamic gradient expansion. Moreover, in the interacting case, due to the presence of nonzero viscosity, for momenta larger than a dissipation scale $k_\theta \gtrsim 1/\Lambda_{\text{sink}}$ (the latter fixed by the viscosity $\Lambda_{\text{sink}} \sim \mathfrak{D}/\theta_{\text{Bragg}} \sim d^2\bar{\rho}$ and by the initial temperature T_0), the power law decay transients to an exponential one, as expected from typical turbulent spectra. As the system under consideration here is not driven, eventually viscous terms take over as time progresses and redistribute smoothly momenta in the (θ, x) space. At times $t \sim t_{\text{Diff}}$, with (see Appendix B for a derivation)

$$t_{\text{Diff}} \equiv \ell^2 m\theta_{\text{Bragg}}/(d^2\bar{\rho}V_0),$$

$$t_{\text{Diff}} \equiv \ell^2 m^2(m - m_0)^2/(m_0^3d^2\bar{\rho}\theta_{\text{Bragg}}), \quad (9)$$

respectively, in the presence of space-dependent trapping potential or space-dependent mass, there is no trace of turbulent behavior any more and the system thermalizes by redistributing a remaining low-momentum density ripple (in

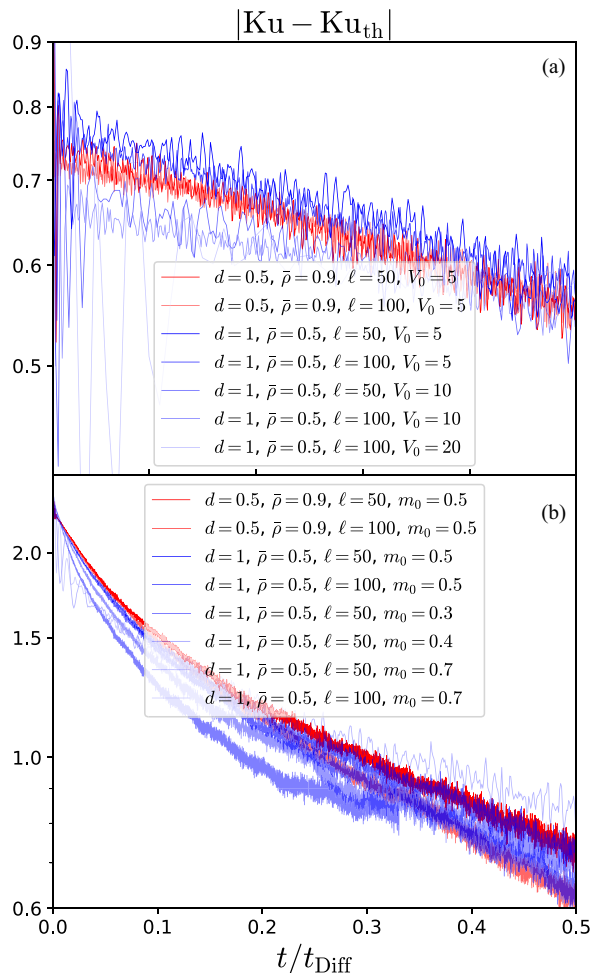


FIG. 4. Kurtosis of the spatially integrated $\rho(\theta, x, t)$ of the exact hard rod gas dynamics with $d = 1$, $\theta_{\text{Bragg}} = 1$, $T_0 = 0.01$, $\ell = L$ and (a) $m_0 = 0$, (b) $V_0 = 0$. The dynamics is shown for different values of d , $\bar{\rho}$, L and (a) V_0 , (b) m_0 . The Log plots show the time evolution as a function of the rescaled time given in Eq. (9): (a) $t/t_{\text{Diff}} \equiv t d^2 \bar{\rho} V_0 / (\theta_{\text{Bragg}} \ell^2)$ and (b) $t/t_{\text{Diff}} \equiv t d^2 \bar{\rho} \theta_{\text{Bragg}} m_0^3 / (m^2 (m - m_0)^2 \ell^2)$. The collapse of the curves is in agreement with the definition of diffusive time scales given in Eq. (9).

x direction) on a time scale set by the minimal diffusion constant in the system (in Fig. 4 are shown plots of kurtosis in rescaled times t/t_{Diff} in the presence of space-dependent trapping potential and space-dependent mass). In this phase, denoted as *diffusively thermalizing phase*, hydrodynamics is restored and gives quantitatively correct prediction for the decay time and the momenta distributions.

It is important to stress again that the inset of the turbulent phase does not signal the breakdown of Euler GHD but rather the *breakdown of hydrodynamic gradient expansion*, so that viscous GHD fails to provide a complete (quantitative) description of the state. As a matter of facts in the free particle case $d = 0$, as shown in Fig. 2, the single particle density experiences a similar turbulent behavior, induced by the fine structures in the phase space generated by the chaotic Euler evolution; however, as in this case Euler hydrodynamics provides an exact description of the dynamics of the system, and all higher derivative terms are always zero, there is clearly no breakdown of the hydrodynamics expansion.

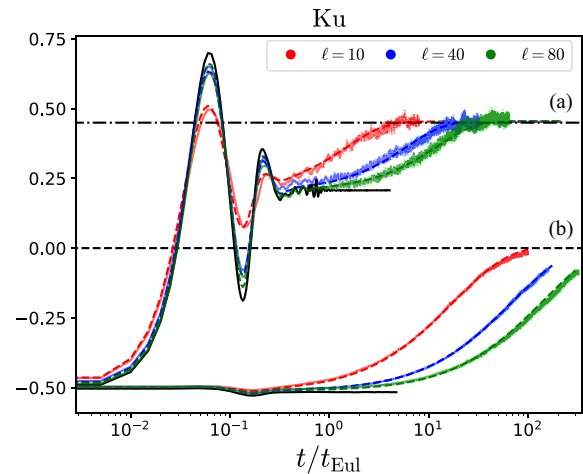


FIG. 5. Comparison of kurtosis of the spatially integrated $\rho(\theta, x, t)$ of the exact HR gas dynamics with $d = 1$, and diffusive GHD prediction for a larger initial temperature $T_0 = 1.0$. Line (a) indicates the kurtosis value of the thermal spatially integrated $\bar{\rho}_{\text{th}}$ corresponding to the case $V_0 = 0$, $m_0 = 0.5$ and line (b) to the case with $V_0 = 0.5$, $m_0 = 0$. Colored dashed lines correspond to the GHD predictions and solid lines for the exact hard rod dynamics (the inviscid Euler hydrodynamics at short times is also reported in black).

Finally, we emphasize that the relevance of such a turbulent regime depends on the initial state. Initial states of the type of Eq. (8) with larger $T_0/\theta_{\text{Bragg}}^2$ ratio, have larger Λ_{sink} and thus a less pronounced turbulent phase and diffusive GHD well reproduces the dynamics at all times, see Fig. 5. Moreover, we also stress the surprising consequence of our results: the GHD description is actually more accurate when ℓ is small, i.e., for strongly broken integrability, as compared with large ℓ , i.e., for weakly broken integrability. Clearly, if ℓ is taken to be very large, the time scale for turbulence $t \sim t_{\text{Eul}} \propto \ell$ and for thermalization $t \sim t_{\text{Diff}} \propto \ell^2$ does increase, but the turbulence phase will be even stronger as ℓ is increased, as diffusion needs longer times to fully redistribute momenta throughout the system.

IV. CONCLUSION

In this letter, we have studied how under the influence of external fields, a system of interacting hard rods thermalizes, a question that has received contradictory answers in the past few years [55,60], and which is extremely relevant in order to understand the thermalization mechanisms for quasi-integrable models.

Our findings are summarized as the following: in the case of smooth (in momentum space) initial states, the evolution of the distribution of momenta remain also smooth both in space and momentum direction, and viscous GHD provides an exact description of the thermalisation dynamics. When instead the distribution develops cusps, a turbulent phase kicks in and the hydrodynamic gradient expansion fails: viscous GHD is not enough to predict the whole thermalisation dynamics, yet it provides a good description of the system at early and, surprisingly enough, late times. Therefore, quite counter-intuitively, viscous GHD predicts more accurately the behavior of a gas with strong external forces rather than one with weak ones.

We stress that our findings here are for generic external forces. The case of exact harmonic confinement, for example, or other potential can present specific features. As turbulence tends to delay the inset of the thermalization time, see Fig. 1, we can expect that the latter can be delayed arbitrarily for specific form of the external force, namely phase II can, in principle, last infinitely (indefinitely), even in the presence of diffusion. We conjecture that this may explain the lack of thermalization observed in the case of harmonic confinement [55,60], and we leave the problem for the near future.

Our work may open new unexplored and exciting directions, in particular on the nature of turbulence and hydrodynamic breaking and restoration in quasi-integrable systems. Indeed, as their effective hydrodynamics is two-dimensional, weaker forms of turbulence, as for example the wave turbulent phase, recently observed in a two-dimensional weakly interacting Bose gas [61–63] and in other quasi-integrable systems in Ref. [64], are therefore possible. This paper provides an example and may open the way for new exciting developments for example within the Lieb-Liniger gas or the Gross-Pitaevskii equation [58,65,66], which could open the way to a possible experimental observation of such a turbulent behavior.

ACKNOWLEDGMENTS

We are grateful to B. Doyon for useful discussions and for explaining how to numerically prepare hard rods GGE states. We thank A. Bastianello, A. De Luca, S. Pappalardi for enlightening discussions and related collaborations. This work has been partially funded by the ERC-2021-STG HEPIQ, Grant No. 101042293.

APPENDIX A: THE HARD RODS ALGORITHM

In this Appendix, we describe the algorithm used to simulate the dynamics of a hard rod gas. We consider a system of N particles $\{P_j, j = 1, \dots, N\}$ having length d and coordinates $\{(x_j, \theta_j), j = 1, \dots, N\}$. They move freely in a one-dimensional space of length L , except for elastic collisions that conserve energy and momentum. The particles are also ordered from left to right $x_{j+1} \geq x_j + d$. The single-particle Hamiltonian of the system is

$$H(\theta, x) = \frac{\theta^2}{2m(x)} + V_1(x), \quad (\text{A1})$$

where $V_1(x)$ is an external trapping potential and $m(x)$ is a space dependent mass. The hard rods algorithm for the time evolution of the system is the following [67]:

- (1) Initialize the system in a GGE state (see Sec. A 1).
- (2) Find the pair of particles $\{P_j, P_{j+1}\}$ that scatter first and their scattering time t_{coll} .
- (3) Let all the particles evolve without interaction until t_{coll} .
- (4) Perform the scattering between particles $\{P_j, P_{j+1}\}$.
- (5) Iterate 1-3.

1. Initialization of the system

We discuss here how to initialize the rods in a GGE state, homogeneous in space and with an arbitrary momentum distribution $h(\theta)$.

In a hard rod GGE state, the distribution of particles in space is a Poisson point process [20,48]. In particular, the probability of finding the edges of two neighboring particles at distance y is equal to

$$\mathbb{P}(y) = \frac{\bar{\rho}}{1 - d\bar{\rho}} e^{-y/\bar{\rho}}, \quad (\text{A2})$$

with $\bar{\rho} = N/L$. In order to impose such statistics, we initialize the system with the following procedure: we place the particle with $j = 1$ at distance $y_1 + d$ from the left border, where y_1 is extracted from a distribution (A2). We repeat for particles with $j > 1$, placing them at position $x_j = x_{j-1} + y_j + d$ until we reach the right border. Then we extract the momentum of particles from the distribution $h(\theta)$. It can be proven that the mean number of particles in the system is actually N .

2. Free particle dynamics and collisional time

The equations of motion for the Hamiltonian defined in Eq. (A1) are

$$\begin{cases} \dot{x} = \frac{\theta}{m(x)}, \\ \dot{\theta} = f_1(x) + \frac{\theta^2}{2} f_2(x), \end{cases} \quad (\text{A3})$$

with $f_1 \equiv -\partial_x V_1(x)$ and $f_2 \equiv -\partial_x m^{-1}(x)$. Considering non-trivial potentials, the system (A3) of nonlinear differential equations is not solvable analytically. Thus, we use a second-order explicit Runge-Kutta method to compute the time evolution of a free particle.

We adopt a time discretization with time step dt and evolve the particle coordinates $\{x_{[n-1]}, \theta_{[n-1]}\} \rightarrow \{x_{[n]}, \theta_{[n]}\}$ according to the equations

$$\begin{aligned} x_{[n]} &= x_{[n-1]} + \frac{K_{v,n}}{m(K_{x,n})} dt, \\ \theta_{[n]} &= \theta_{[n-1]} + \left(f_1(K_{x,n}) + f_2(K_{x,n}) \frac{K_{v,n}^2}{2} \right) dt, \\ K_{x,n} &\equiv x_{[n-1]} + \frac{\theta_{[n-1]} dt}{m(x_{[n-1]}) 2}, \\ K_{v,n} &\equiv \theta_{[n-1]} + \left(f_1(x_{[n-1]}) + f_2(x_{[n-1]}) \frac{\theta_{[n-1]}^2}{2} \right) \frac{dt}{2}, \end{aligned} \quad (\text{A4})$$

where $\{x_{[n]}, \theta_{[n]}\}$ is the Runge-Kutta approximation of $\{x(t_n), \theta(t_n)\}$ with $t_n = n dt$. According to Eq. (A4), the collisional time between two neighboring particles $\{P_j, P_{j+1}\}$ is

$$t_{\text{coll}}^j = \frac{d - (x_{j+1} - x_j)}{\theta_{j+1}/m(x_{j+1}) - \theta_j/m(x_j)} + \mathcal{O}(dt^2). \quad (\text{A5})$$

Hence, at each time step, we evaluate the minimal collisional time $t_{\text{coll}} = \{\min t_{\text{coll}}^j, j = 1, \dots, N-1\}$ between particles. As long as $t_{\text{coll}} > dt$ is valid, we perform the Runge-Kutta time evolution using Eqs. (A4) with time step dt . When $t_{\text{coll}} < dt$, we perform the Runge-Kutta time evolution with time step t_{coll} and then we perform the collision.

3. Collisions between particles

In the HR gas, the particles experience contact interaction that conserves energy and momentum. Hence, two rods $\{P_j, P_{j+1}\}$ interact only if $x_{j+1} = x_j + d$.

Considering the scattering between particles $\{P_j, P_{j+1}\}$ with initial coordinates $\{x_j, \theta_j\}$, $\{x_{j+1} = x_j + d, \theta_{j+1}\}$, their momenta after the collision will be

$$\begin{aligned}\theta_{j+1}^f &= \frac{2m(x_{j+1})\theta_j - m(x_j)\theta_{j+1} + m(x_{j+1})\theta_{j+1}}{m(x_j) + m(x_{j+1})}, \\ \theta_j^f &= \frac{2m(x_j)\theta_{j+1} - m(x_{j+1})\theta_j + m(x_j)\theta_j}{m(x_j) + m(x_{j+1})}.\end{aligned}\quad (\text{A6})$$

Thus, in the case of constant mass $m(x) = m_0$, the particles simply exchange their momenta through collisions.

APPENDIX B: THE GHD EQUATION FOR A HARD ROD GAS WITH FORCES

In this Appendix, we introduce the GHD theory for a HR gas in the presence of external forces. In particular, we consider a one-dimensional gas of hard rods with length d and in the presence of the external trapping potential $V_1(x)$ and with a space-dependent mass $m(x)$ such that the bare energy and momentum of a single particle are defined as

$$\epsilon(\theta, x) = \frac{\theta^2}{2m(x)} + V_1(x), \quad p(\theta, x) = \theta. \quad (\text{B1})$$

In the absence of external potentials, the system is clearly integrable [19–21] and it has been proven that at large scale it is described by GHD [23,24]. In Sec. B 1 we define the dressing operator for the hard rod gas, and we describe the GHD at the Euler scale. In Sec. B 2 we define the full GHD equation with viscosities and force terms of the system.

1. The GHD equation at Euler scale

We consider an ensemble of hard rods moving in one dimension with velocities v . The quasiparticles are identified with trajectory tracers, following the centers of particles. Whenever two particles collide, the two tracers associated with them, exchange their position. Thus, they compute an instantaneous displacement of d in space, with d equal to the length of the rods. The momenta θ of the quasiparticles can be identified with the velocities v of the particles. Hence, we can define a local stationary state via the local density of quasiparticles $\rho(\theta, x, t)$ so that $\rho(\theta, x, t)dx d\theta$ is equal to the number of particles in the phase space interval $[(x, x + dx), (\theta, \theta + d\theta)]$.

Since the spatial displacement of the quasiparticles at each collision is not dependent on their momenta, the scattering kernel (in real space) is particularly simple

$$T_x(\theta, \theta') = -\frac{d}{2\pi}. \quad (\text{B2})$$

Given the scattering kernel (B2), we can define the dressing operation for single-particle functions $f(\theta, x)$

$$f^{\text{dr}}(\theta, x) = f(\theta, x) - d \int_{\mathbb{R}} d\theta' \rho(\theta, x, t) f(\theta', x). \quad (\text{B3})$$

Thus, if we use the dressing operation on the identity we have

$$1^{\text{dr}} = 1 - \bar{\rho}(x, t)d \quad \text{with} \quad \bar{\rho}(x, t) \equiv \int_{\mathbb{R}} d\theta \rho(\theta, x, t). \quad (\text{B4})$$

The effective velocity $v^{\text{eff}}(\theta, x)$ of a quasiparticle is defined by [68]

$$v_{[\rho]}^{\text{eff}}(\theta, x) \equiv \frac{(\partial_\theta \epsilon)^{\text{dr}}}{(\partial_\theta p)^{\text{dr}}}, \quad (\text{B5})$$

and the effective acceleration $a^{\text{eff}}(\theta, x)$ is defined by

$$a_{[\rho]}^{\text{eff}}(\theta, x) \equiv \frac{(-\partial_x \epsilon)^{\text{dr}}}{(\partial_\theta p)^{\text{dr}}}. \quad (\text{B6})$$

Using the explicit form of the single-particle energy and momentum (B1) and the dressing operation (B3), we get the expressions for the effective velocity and acceleration for a HR gas

$$v_{[\rho]}^{\text{eff}}(\theta, x, t) = \frac{\theta - d \int_{\mathbb{R}} d\theta' \theta' \rho(\theta', x, t)}{m(x)(1 - \bar{\rho}(x, t)d)}, \quad (\text{B7})$$

$$a_{[\rho]}^{\text{eff}}(\theta, x, t) = f_1(x) + f_2(x) \frac{\frac{\theta^2}{2} - d \int_{\mathbb{R}} d\theta' \frac{\theta'^2}{2} \rho(\theta', x, t)}{1 - \bar{\rho}(x, t)d}, \quad (\text{B8})$$

where we defined $f_1 = -\partial_x V_1(x)$ and $f_2 = -\partial_x m^{-1}(x)$. The expressions (B7) and (B8) are equivalent to the components of the flow vector \mathbf{J}^{eff} defined in the main text.

Thus, the GHD equation at the Euler scale reads

$$\begin{aligned}\partial_t \rho(\theta, x, t) + \partial_x (v_{[\rho]}^{\text{eff}}(\theta, x, t) \rho(\theta, x, t)) \\ + \partial_\theta (a_{[\rho]}^{\text{eff}}(\theta, x, t) \rho(\theta, x, t)) = 0.\end{aligned}\quad (\text{B9})$$

2. The diffusive GHD equation with forces

In this section, we take into consideration the second-order terms in the hydrodynamic expansion. The diffusive GHD equation in the main text can be written as [49,69]

$$\begin{aligned}\partial_t \rho + \partial_x (v_{[\rho]}^{\text{eff}} \rho) + \partial_\theta (a_{[\rho]}^{\text{eff}} \rho) \\ = \frac{1}{2} [\partial_x (\mathfrak{D}_{[\rho]}^{(1,1)} \partial_x \rho) + \partial_x (\mathfrak{D}_{[\rho]}^{(1,2)} \partial_\theta \rho) \\ + \partial_\theta (\mathfrak{D}_{[\rho]}^{(2,1)} \partial_x \rho) + \partial_\theta (\mathfrak{D}_{[\rho]}^{(2,2)} \partial_\theta \rho)],\end{aligned}\quad (\text{B10})$$

where the diffusion matrices $\mathfrak{D}_{[\rho]}$ is a 2×2 matrix of operators defined as

$$\begin{aligned}\mathfrak{D}_{[\rho]}(\theta, \theta') = d^2 \left(\delta_{\theta, \theta'} \int_{\mathbb{R}} d\kappa \rho(\kappa, x, t) \mathbf{g}(\theta, \kappa) \right. \\ \left. - \rho(\theta, x, t) \mathbf{g}(\theta, \theta') \right),\end{aligned}\quad (\text{B11})$$

with $\delta_{\theta, \theta'}$ Dirac delta. We also defined the kernels $\mathbf{g}(\theta, \theta')$ as

$$\frac{\mathbf{g}}{d^2} = \begin{pmatrix} |v_{[\rho]}^{\text{eff}}(\theta) - v_{[\rho]}^{\text{eff}}(\theta')| & \xi_{\theta, \theta'} (a_{[\rho]}^{\text{eff}}(\theta) - a_{[\rho]}^{\text{eff}}(\theta')) \\ \xi_{\theta, \theta'} (a_{[\rho]}^{\text{eff}}(\theta) - a_{[\rho]}^{\text{eff}}(\theta')) & \frac{(a_{[\rho]}^{\text{eff}}(\theta) - a_{[\rho]}^{\text{eff}}(\theta'))^2}{|v_{[\rho]}^{\text{eff}}(\theta) - v_{[\rho]}^{\text{eff}}(\theta')|} \end{pmatrix}. \quad (\text{B12})$$

3. Euler and diffusive time scales

Here we consider a system of hard rods prepared in a homogeneous state with distribution of momenta given by

two two Gaussian peaks centered in $\theta = \pm\theta_{\text{Bragg}}$ and with a given initial temperature T_0 . Since rapidities have the same units as momentum, the unit of velocity is $v \sim \theta_{\text{Bragg}}/m$. The macroscopic length scale of the system is the parameter ℓ , defining the potential trap and the space dependent mass. Then, the Euler time scale is given by the macroscopic unit of length and velocity: $t_{\text{Eul}} = m\ell/\theta_{\text{Bragg}}$.

To compute the diffusive time scale we firstly consider the case with $m_0 = 0$ and $V_0 \neq 0$. In this case, from GHD equation, we know that the diffusive time scale is inversely proportional to the force $F \sim V_0/\ell$ and to the diffusive kernel $\mathfrak{D}_{[\rho]}^{(x,x)} \sim d^2\bar{\rho}/m$. Since $[\mathfrak{D}_{[\rho]}^{(x,x)}V_0/\ell]^{-1} = [t^2/\ell^2]$, then the only time scale that we can define using these quantities, together with the unit of velocity and length, is

$$t_{\text{Diff}} = \frac{\theta_{\text{Bragg}}\ell^2}{d^2\bar{\rho}V_0}. \quad (\text{B13})$$

Now we consider the case with $V_0 = 0$ and $m_0 \neq 0$. Again, the diffusive time scale is known to be inversely proportional to the force $F \sim \mathfrak{f}_2\theta^2$ and to the diffusive kernel $\mathfrak{D}_{[\rho]}^{(\theta,\theta)} \sim d^2\bar{\rho}m(x)\mathfrak{f}_2^2\theta_{\text{Bragg}}^2$. Since $[\mathfrak{D}_{[\rho]}^{(x,\theta)}\mathfrak{f}_2\theta^2]^{-1} = [t^4/m^2\ell^2]$, the only time scale that we can define using this quantity, together with the unit of velocity and length, is $t_{\text{Diff}} = (d^2\bar{\rho}\ell m(x)^2\mathfrak{f}_2^3\theta_{\text{Bragg}}^3)^{-1}$. Using that $(m^2(x)\mathfrak{f}_2^2)^{-1} \sim \ell^3 m^2(m - m_0)^2/m_0^3$ we can express the diffusive time scale in terms of m_0

$$t_{\text{Diff}} = \frac{\ell^2 m^2(m - m_0)^2}{d^2\bar{\rho}\theta_{\text{Bragg}} m_0^3}. \quad (\text{B14})$$

APPENDIX C: STATIONARITY OF THERMAL DISTRIBUTION UNDER DIFFUSIVE GHD

In this Appendix, we show that the thermal distribution is stationary under diffusive GHD. Namely, we prove that the thermal distribution $\rho_{\text{th}}(\theta, x)$ is a solution of the equation,

$$\begin{aligned} & -\partial_x(v_{[\rho_{\text{th}}]}^{\text{eff}}\rho_{\text{th}}) - \partial_\theta(a_{[\rho_{\text{th}}]}^{\text{eff}}\rho_{\text{th}}) + \frac{1}{2}[\partial_x(\mathfrak{D}_{[\rho_{\text{th}}]}^{(1,1)}\partial_x\rho_{\text{th}}) \\ & + \partial_x(\mathfrak{D}_{[\rho_{\text{th}}]}^{(1,2)}\partial_\theta\rho_{\text{th}}) + \partial_\theta(\mathfrak{D}_{[\rho_{\text{th}}]}^{(2,1)}\partial_x\rho_{\text{th}}) + \partial_\theta(\mathfrak{D}_{[\rho_{\text{th}}]}^{(2,2)}\partial_\theta\rho_{\text{th}})] \\ & = 0. \end{aligned} \quad (\text{C1})$$

In order to do that we introduce some explicit expressions for the derivatives of a thermal distribution. This latter is defined via the function

$$\begin{aligned} \epsilon_{\text{th}}(\theta) &= \beta w(\theta; x) - \mu + \frac{d}{2\pi} \int d\theta e^{-\epsilon_{\text{th}}(\theta)} \\ w(\theta, x) &= \frac{\theta^2}{2m(x)} + V_1(x), \end{aligned} \quad (\text{C2})$$

as $n_{\text{th}}(\theta) = e^{-\epsilon_{\text{th}}(\theta)}$ at each point x . It satisfies the relations

$$\begin{aligned} \partial_x n_{\text{th}} &= (1 - d\bar{\rho}_{\text{th}})\beta\mathfrak{f}_1 n_{\text{th}} + \beta\mathfrak{f}_2 n_{\text{th}} \left(\frac{\theta^2}{2} - d\bar{e}_{\text{th}} \right), \\ \partial_\theta n_{\text{th}} &= -\beta\theta n_{\text{th}}/m(x), \\ \partial_x \rho_{\text{th}} &= -\frac{d\partial_x \bar{\rho}_{\text{th}}}{(1 - d\bar{\rho}_{\text{th}})} \rho_{\text{th}} + (1 - d\bar{\rho}_{\text{th}})\beta\mathfrak{f}_1 \rho_{\text{th}} \\ &+ \beta\mathfrak{f}_2 \rho_{\text{th}} \left(\frac{\theta^2}{2} - d\bar{e}_{\text{th}} \right), \\ \partial_\theta \rho_{\text{th}} &= -\beta\theta \rho_{\text{th}}/m(x), \\ \partial_x \bar{\rho}_{\text{th}} &= (1 - d\bar{\rho}_{\text{th}})^2 (\beta\mathfrak{f}_1 \bar{\rho}_{\text{th}} + \beta\mathfrak{f}_2 \bar{e}_{\text{th}}), \end{aligned} \quad (\text{C3})$$

with $\bar{e}_{\text{th}} \equiv \int d\theta \rho_{\text{th}}(\theta)\theta^2/2$ and $\bar{u}_{\text{th}} \equiv \int d\theta \theta \rho_{\text{th}}(\theta) = 0$.

Firstly, we derive the explicit expressions for the Euler terms in Eq. (C1) using the formulas (C3)

$$\begin{aligned} \partial_x(v_{[\rho_{\text{th}}]}^{\text{eff}}\rho_{\text{th}}) &= \partial_x(\theta n_{\text{th}}/m(x)) \\ &= \theta(\partial_x n_{\text{th}})/m(x) - \theta\mathfrak{f}_2 n_{\text{th}} \\ &= -\mathfrak{f}_1 \partial_\theta \rho_{\text{th}} + \beta\mathfrak{f}_2 \theta \left(\frac{\theta^2}{2} - d\bar{e}_{\text{th}} \right) n_{\text{th}}/m(x) - \theta\mathfrak{f}_2 n_{\text{th}}, \end{aligned} \quad (\text{C4})$$

$$\begin{aligned} \partial_\theta(a_{[\rho_{\text{th}}]}^{\text{eff}}\rho_{\text{th}}) &= \mathfrak{f}_1 \partial_\theta \rho_{\text{th}} - \beta\mathfrak{f}_2 \theta \left(\frac{\theta^2}{2} - d\bar{e}_{\text{th}} \right) n_{\text{th}}/m(x) + \theta\mathfrak{f}_2 n_{\text{th}} \\ &= -\partial_x(\rho_{\text{th}} v_{[\rho_{\text{th}}]}^{\text{eff}}), \end{aligned} \quad (\text{C5})$$

hence, the thermal distribution is stationary under Euler GHD. Then we take into consideration the diffusive terms of Eq. (C1), as follows:

$$\mathfrak{D}_{[\rho_{\text{th}}]}^{(1,1)}\partial_x \rho_{\text{th}} = \int_{\mathbb{R}} d\theta' [\rho_{\text{th}}(\theta') \mathfrak{g}_{\theta, \theta'}^{(1,1)} \partial_x \rho_{\text{th}}(\theta) - \rho_{\text{th}}(\theta) \mathfrak{g}_{\theta, \theta'}^{(1,1)} \partial_x \rho_{\text{th}}(\theta')] = \frac{d^2\beta\mathfrak{f}_2}{m(x)(1 - d\bar{\rho}_{\text{th}})} \int_{\mathbb{R}} d\theta' |\theta - \theta'| \left(\frac{\theta^2}{2} - \frac{\theta'^2}{2} \right) \rho_{\text{th}}(\theta) \rho_{\text{th}}(\theta'), \quad (\text{C6})$$

$$\begin{aligned} \mathfrak{D}_{[\rho_{\text{th}}]}^{(1,2)}\partial_\theta \rho_{\text{th}} &= \int_{\mathbb{R}} d\theta' [\rho_{\text{th}}(\theta') \mathfrak{g}_{\theta, \theta'}^{(1,2)} \partial_\theta \rho_{\text{th}}(\theta) - \rho_{\text{th}}(\theta) \mathfrak{g}_{\theta, \theta'}^{(1,2)} \partial_\theta \rho_{\text{th}}(\theta')] \\ &= -\frac{d^2\beta\mathfrak{f}_2}{m(x)(1 - d\bar{\rho}_{\text{th}})} \int_{\mathbb{R}} d\theta' |\theta - \theta'| \left(\frac{\theta^2}{2} - \frac{\theta'^2}{2} \right) \rho_{\text{th}}(\theta) \rho_{\text{th}}(\theta') \\ &= -\mathfrak{D}_{[\rho_{\text{th}}]}^{(1,1)}\partial_x \rho_{\text{th}}, \end{aligned} \quad (\text{C7})$$

$$\begin{aligned} \mathfrak{D}_{[\rho_{\text{th}}]}^{(2,1)}\partial_x \rho_{\text{th}} &= \int_{\mathbb{R}} d\theta' [\rho_{\text{th}}(\theta') \mathfrak{g}_{\theta, \theta'}^{(2,1)} \partial_x \rho_{\text{th}}(\theta) - \rho_{\text{th}}(\theta) \mathfrak{g}_{\theta, \theta'}^{(2,1)} \partial_x \rho_{\text{th}}(\theta')] \\ &= \frac{d^2\beta\mathfrak{f}_2^2}{(1 - d\bar{\rho}_{\text{th}})} \int_{\mathbb{R}} d\theta' \text{sgn}(\theta - \theta') \left(\frac{\theta^2}{2} - \frac{\theta'^2}{2} \right)^2 \rho_{\text{th}}(\theta) \rho_{\text{th}}(\theta'), \end{aligned} \quad (\text{C8})$$

$$\begin{aligned}
\mathfrak{D}_{[\rho_{\text{th}}]}^{(2,2)} \partial_{\theta} \rho_{\text{th}} &= \int_{\mathbb{R}} d\theta' [\rho_{\text{th}}(\theta') \mathfrak{g}_{\theta, \theta'}^{(2,2)} \partial_{\theta} \rho_{\text{th}}(\theta) - \rho_{\text{th}}(\theta) \mathfrak{g}_{\theta, \theta'}^{(2,2)} \partial_{\theta} \rho_{\text{th}}(\theta')] \\
&= -\frac{d^2 \beta \mathfrak{f}_2^2}{(1 - d\bar{\rho}_{\text{th}})} \int_{\mathbb{R}} d\theta' \text{sgn}(\theta - \theta') \left(\frac{\theta^2}{2} - \frac{\theta'^2}{2} \right)^2 \rho_{\text{th}}(\theta) \rho_{\text{th}}(\theta') \\
&= -\mathfrak{D}_{[\rho_{\text{th}}]}^{(2,1)} \partial_x \rho_{\text{th}},
\end{aligned} \tag{C9}$$

where we used the relations (C3) and the symmetry of the operators $\mathfrak{D}_{[\rho]}^{(i,j)}$ with $i, j \in \{1, 2\}$.

Thus, we proved that the thermal distribution is stationary also under the diffusive terms of GHD equation

$$\partial_x (\mathfrak{D}_{[\rho_{\text{th}}]}^{(1,1)} \partial_x \rho_{\text{th}} + \mathfrak{D}_{[\rho_{\text{th}}]}^{(1,2)} \partial_{\theta} \rho_{\text{th}}) + \partial_{\theta} (\mathfrak{D}_{[\rho_{\text{th}}]}^{(2,1)} \partial_x \rho_{\text{th}} + \mathfrak{D}_{[\rho_{\text{th}}]}^{(2,2)} \partial_{\theta} \rho_{\text{th}}) = 0. \tag{C10}$$

APPENDIX D: KINETIC PICTURE OF GHD EQUATION

The aim of this Appendix is to give a kinetic interpretation of GHD equation. In Sec. D1, we derive the Euler GHD equation in the presence of external forces using only kinetic arguments. Next, in Sec. D2, we give a kinetic interpretation of the diffusive terms of Eq. (B10) as diffusive corrections to ballistic quasiparticle spreading.

1. Kinetic derivation of Euler GHD equation

In this section, we extend the argument presented in [20] to derive the Euler GHD equation in the presence of external forces. We consider a system of hard rods of length d . The one-particle Hamiltonian of the system is

$$H(\theta, x) = \frac{\theta^2}{2m(x)} + V_1(x), \tag{D1}$$

with $V_1(x)$ external trapping potential and $m(x)$ space dependent mass. The Hamilton equations associated to (D1) are

$$\begin{aligned}
\dot{x} &= \frac{\theta}{m(x)}, \\
\dot{\theta} &= \mathfrak{f}_1(x) + \frac{\theta^2}{2} \mathfrak{f}_2(x),
\end{aligned} \tag{D2}$$

where we defined $\mathfrak{f}_1 \equiv -\partial_x V_1(x)$ and $\mathfrak{f}_2 \equiv -\partial_x m^{-1}(x)$. Considering the system in the thermodynamic limit, we introduce $\rho(\theta, x, t)$ as the average particle density of the gas, namely $\rho(\theta, x, t) dx d\theta dt$ is equal to the number of particles in the interval $[(x, x + dx), (\theta, \theta + d\theta), (t, t + dt)]$. The total particle density is given by

$$\bar{\rho}(x, t) = \int_{\mathbb{R}} d\theta \rho(\theta, x, t). \tag{D3}$$

The particles are also labeled to exchange their position during the elastic collisions. Namely, each particle moves freely, according to Eq. (D2), except for jumps in position and momentum at each collision [20,23]. On a time scale much larger than the mean free time, the particles will move with an effective velocity and effective acceleration that depend on all the collisions that they make. In particular, each time a particle collides from the left (right) with another one, its position is shifted to the right (left) by d . Hence, the effective velocity of a particle having momentum θ must be equal to

$$v^{\text{eff}}(\theta, x, t) = \frac{\theta}{m(x)} + d \int_{\mathbb{R}} d\theta' (n_+(\theta, \theta') - n_-(\theta, \theta')), \tag{D4}$$

where $n_{+(-)}(\theta, \theta') dt d\theta'$ is the probability of a particle with momentum θ making a scattering with a particle with mo-

mentum in $[\theta', \theta' + d\theta']$ from right (left) in the time step $[t, t + dt]$. The average distance $\bar{d}(x, t)$ between particles in the interval $[(x, x + dx), (t, t + dt)]$ is given by the ratio between the total free space and the total number of particles,

$$\bar{d}(x, t) = \frac{dx dt - d\bar{\rho}(x, t) dx dt}{\bar{\rho}(x, t) dx dt} = \frac{1 - d\bar{\rho}(x, t)}{\bar{\rho}(x, t)}. \tag{D5}$$

The probability of the particle firstly colliding with another one having velocity in the range $[\theta', \theta' + d\theta']$ is $(\rho(\theta', x, t)/\bar{\rho}(x, t)) d\theta'$. Thus, assuming that the space-dependent mass $m(x)$ is slowly varying compared to the dimension d of the rods, the probability of having this scattering in the time interval $[t, t + dt]$ is equal to

$$\begin{aligned}
&d(n_+(\theta, \theta') - n_-(\theta, \theta')) dt d\theta' \\
&= d \frac{\rho(\theta', x, t)}{\bar{\rho}(x, t)} d\theta' \frac{(\theta/m(x) - \theta'/m(x + d))}{\bar{d}(x, t)} dt \\
&= d \frac{\rho(\theta', x, t)}{m(x)(1 - d\bar{\rho}(x, t))} (\theta - \theta') dt d\theta' + \mathcal{O}(d\partial_x m^{-1}(x)).
\end{aligned} \tag{D6}$$

Using the probability (D6) in Eq. (D4) we get the explicit expression for the effective velocity

$$v^{\text{eff}}(\theta, x, t) = \frac{\theta}{m(x)} + d \int_{\mathbb{R}} d\theta' \frac{\rho(\theta', x, t)(\theta - \theta')}{m(x)(1 - d\bar{\rho}(x, t))}, \tag{D7}$$

which is equal to the one previously shown in Eq. (B7). The effective acceleration is expected to have a similar form as (D4), but with a different kernel $T_{\theta}(\theta, \theta')$ defined as the jump of momenta at each scattering,

$$\begin{aligned}
&a^{\text{eff}}(\theta, x, t) \\
&= a^{\text{br}}(\theta, x) + \int_{\mathbb{R}} d\theta' T_{\theta}(\theta, \theta') (n_+(\theta, \theta') - n_-(\theta, \theta')) \\
&= a^{\text{br}}(\theta, x) + \int_{\mathbb{R}} d\theta' T_{\theta}(\theta, \theta') \frac{\rho(\theta', x, t)(\theta - \theta')}{m(x)(1 - d\bar{\rho}(x, t))},
\end{aligned} \tag{D8}$$

where $a^{\text{br}}(\theta, x) \equiv \mathfrak{f}_1(x) + \frac{\theta^2}{2} \mathfrak{f}_2(x)$ is the bare acceleration shown in Eq. (D2). We now derive an explicit expression for the kernel $T_{\theta}(\theta, \theta')$. Since the collisions are elastic, they conserve energy and momentum of the two particles that are colliding. Thus, if a particle of momentum θ collides with a particle with θ' , its final momentum will be

$$\theta^{\text{f}} = \frac{2m(x + d)\theta - m(x)\theta' + m(x + d)\theta'}{m(x + d) + m(x)}. \tag{D9}$$

Assuming that $m^{-1}(x)$ is slow varying compared to the dimension d of the rods, we can expand it in derivatives: $m^{-1}(x+d) = m^{-1}(x) - d\mathfrak{f}_2(x) + \mathcal{O}(d^2\partial_x^2 m^{-1}(x))$. Hence, the series expansion of $m(x+d)$ around $d=0$ is

$$\begin{aligned} \frac{m(x+d)}{m(x)} &= 1 + d\mathfrak{f}_2(x)m(x) \\ &+ \mathcal{O}(d^2(\partial_x m^{-1})^2/m(x), d^2(\partial_x^2 m^{-1})/m(x)). \end{aligned} \quad (\text{D10})$$

Expanding up to first order the Eq. (D9) we get

$$\begin{aligned} \theta^f &= \theta + d\mathfrak{f}_2 m(x)(\theta' + \theta) \\ &+ \mathcal{O}(d^2(\partial_x m^{-1})^2/m, d^2\partial_x^2 m^{-1}/m). \end{aligned} \quad (\text{D11})$$

Thus, from the linearization (D11) of Eq. (D9) we can express the scattering kernel in momentum space as

$$T_\theta(\theta, \theta') \equiv \theta^f - \theta \simeq d\mathfrak{f}_2 m(x) \frac{\theta' + \theta}{2}. \quad (\text{D12})$$

Finally, using the formula (D12) in the effective acceleration (D8) we get

$$a^{\text{eff}}(\theta, x, t) = a^{\text{br}}(\theta, x) + d\mathfrak{f}_2(x) \int_{\mathbb{R}} d\theta' \frac{\rho(\theta', x, t)}{1 - d\bar{\rho}(x, t)} \left(\frac{\theta^2}{2} - \frac{\theta'^2}{2} \right) = \mathfrak{f}_1(x) + \mathfrak{f}_2(x) \frac{\theta^2/2 - d \int d\theta' \rho(\theta', x, t) \theta'^2/2}{1 - d\bar{\rho}(x, t)}, \quad (\text{D13})$$

which is equal to the formula (B8).

Now we impose the local conservation of mass on a fluid cell which is initially at time t in the interval $[(x, x+dx), (\theta, \theta+d\theta)]$ [20]. After a time step dt , the initial interval is transformed into $[(x+v^{\text{eff}}(\theta, x, t)dt, x+dx+v^{\text{eff}}(\theta, x, t)dt), (\theta+a^{\text{eff}}(\theta, x, t)dt, \theta+d\theta+a^{\text{eff}}(\theta, x, t)dt)]$. Imposing the conservation of mass, we find the equation

$$\begin{aligned} \rho(\theta, x, t)dx d\theta &= \rho(\theta + a^{\text{eff}}(\theta, x, t)dt, x + v^{\text{eff}}(\theta, x, t)dt, t + dt)[dx + v^{\text{eff}}(x + d\theta, x, t)dt - v^{\text{eff}}(\theta, x, t)dt] \\ &\times [d\theta + a^{\text{eff}}(\theta, x + d\theta, t)dt - a^{\text{eff}}(\theta, x, t)dt], \end{aligned} \quad (\text{D14})$$

where v^{eff} and a^{eff} are defined in Eq. (D7) and (D13). Taking into consideration only first-order terms we get

$$\begin{aligned} &\frac{\rho(\theta, x, t + dt) - \rho(\theta, x, t)}{dt} + v^{\text{eff}}(\theta, x, t) \frac{\rho(\theta, x + v^{\text{eff}}(\theta, x, t)dt, t) - \rho(\theta, x, t)}{v^{\text{eff}}(\theta, x, t)dt} \\ &+ a^{\text{eff}}(\theta, x, t) \frac{\rho(\theta + a^{\text{eff}}(\theta, x, t)dt, x, t) - \rho(\theta, x, t)}{a^{\text{eff}}(\theta, x, t)dt} \\ &+ \rho(\theta, x, t) \left(\frac{v^{\text{eff}}(\theta + d\theta, x, t) - v^{\text{eff}}(\theta, x, t)}{dx} + \frac{a^{\text{eff}}(\theta + d\theta, x, t) - a^{\text{eff}}(\theta, x, t)}{d\theta} \right) = 0. \end{aligned} \quad (\text{D15})$$

Hence, the Eq. (D15) is formally identical to the Euler GHD equation

$$\partial_t \rho(\theta, x, t) + \partial_x (v^{\text{eff}}(\theta, x, t) \rho(\theta, x, t)) + \partial_\theta (a^{\text{eff}}(\theta, x, t) \rho(\theta, x, t)) = 0. \quad (\text{D16})$$

2. Diffusive corrections to ballistic quasiparticle spreading

The purpose of this section is to give a kinetic interpretation of the diffusive terms of Eq. (B10) as diffusive corrections to ballistic particle spreading. In particular, we will generalize the argument presented in [50] in the case of a system with free particle Hamiltonian (D1).

We consider the trajectory $(x(t), \theta(t))$ of a single particle on the phase space. At the leading order, the particle moves ballistically with $(\dot{x}(t), \dot{\theta}(t)) \simeq (v^{\text{eff}}(\theta, x), a^{\text{eff}}(\theta, x))$, where the physical interpretation of these relations is explained in Appendix D1. Since this ballistic spreading depends on the interaction with the other particles in the system, it is subjected to a diffusive broadening due to the fluctuations of the statistical ensemble [50].

Our aim is to compute the variance of the fluctuations $\mathbf{R} \equiv (\delta x, \delta \theta)$ of the quasiparticle's trajectory in the phase space induced by a fluctuation in the density of particles at (θ', x) . Namely, we want to compute

$$\begin{aligned} &\langle \mathbf{R} \otimes \mathbf{R}(\theta, x, t) \rangle^c |_{\theta'} \\ &= \begin{pmatrix} \langle \delta x^2(\theta, x, t) \rangle^c |_{\theta'} & \langle \delta x \delta \theta(\theta, x, t) \rangle^c |_{\theta'} \\ \langle \delta x \delta \theta(\theta, x, t) \rangle^c |_{\theta'} & \langle \delta \theta^2(\theta, x, t) \rangle^c |_{\theta'} \end{pmatrix}, \end{aligned} \quad (\text{D17})$$

where we defined $\langle \bullet \rangle^c$ as the connected part of the average over the GGE. Let us first consider the space variance and express it in terms of density fluctuations

$$\begin{aligned} \langle \delta x^2(\theta, x, t) \rangle^c |_{\theta'} &= t^2 \langle (\delta v^{\text{eff}})^2 \rangle^c |_{\theta'} \\ &= t^2 \left(\frac{\delta v^{\text{eff}}(\theta)}{\delta n(\theta')} \right)^2 \langle \delta n(\theta')^2 \rangle^c, \end{aligned} \quad (\text{D18})$$

where $n(\theta, x, t)$ denote the generalized Fermi factor, that for the Hard Rod system is $n(\theta, x, t) = \rho(\theta, x, t)/(1 - \bar{\rho}(x, t)d)$ [68]. The density fluctuations of a GGE state, computed over an interval of length Λ , are diagonal in position and momentum [50,70] and for the hard rod gas are equal to [23]

$$\begin{aligned} \langle \delta n(\theta, x) \delta n(\theta', x') \rangle^c &\equiv \langle n(\theta, x) n(\theta', x') \rangle - \langle n(\theta, x) \rangle \langle n(\theta', x') \rangle \\ &= \delta(x - x') \delta(\theta - \theta') \frac{n(\theta, x)}{\Lambda(1 - a\bar{\rho}(x))}. \end{aligned} \quad (\text{D19})$$

Since the collisions between quasiparticles with momenta θ and θ' can happen only inside the light-cone defined by the velocity $v^{\text{eff}}(\theta) - v^{\text{eff}}(\theta')$, the fluctuations must be computed over the region of length $\Lambda = t|v^{\text{eff}}(\theta) - v^{\text{eff}}(\theta')|$. The

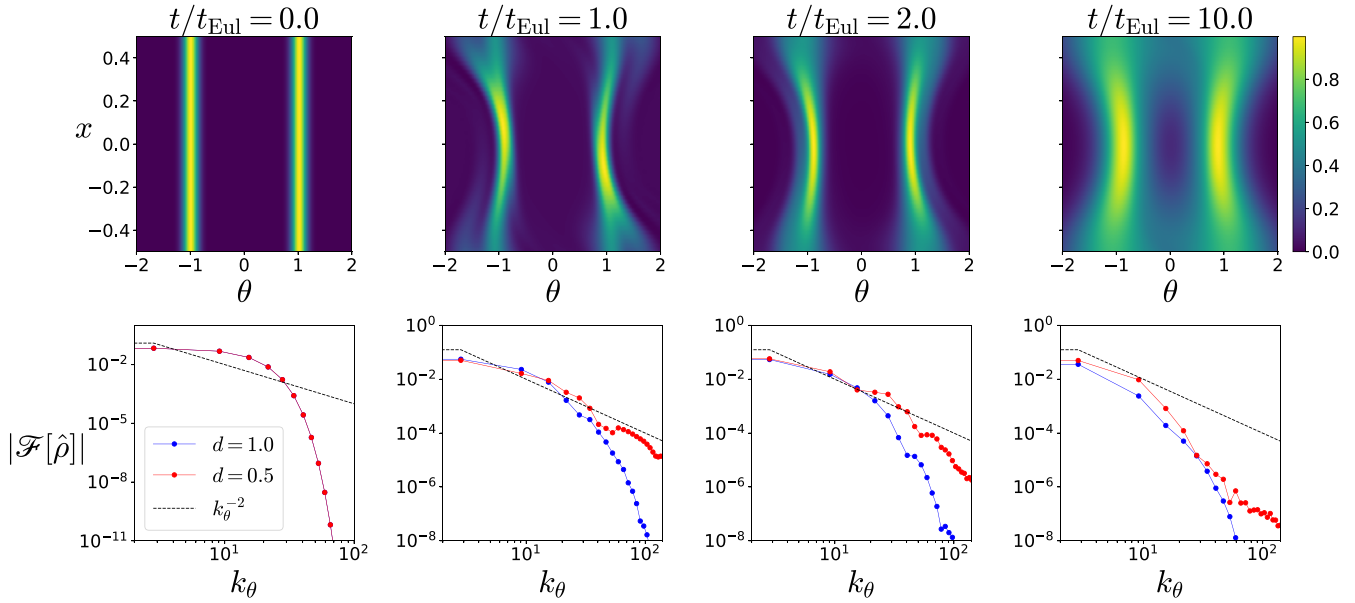


FIG. 6. GHD evolution with $m_0(x) = 0.5$ and $V_0 = 0$ and $\ell = 80$, initialized in a Bragg pulse state with $T_0 = 0.01$: (top) density plot of the density $\rho(\theta, x, t)$ as function of momentum θ and position x at different times, for rods with length $d = 1$. (bottom) Log-Log plot of the absolute value of the Fourier transform in θ of the spatially integrated density as a function of Fourier vector k_θ and two different values of the rods' length d . The behavior of the system, in this case, is qualitatively the same as the one shown in Fig. 3 of the main text.

derivative of the effective velocity with respect to the generalized Fermi factor can be computed from Eq. (B5) and is equal to

$$\frac{\delta v^{\text{eff}}(x, \theta, t)}{\delta n(x, \theta', t)} = d(1 - \bar{\rho}(x, t)d)(v^{\text{eff}}(\theta, x, t) - v^{\text{eff}}(\theta', x, t)). \quad (\text{D20})$$

Hence, using the relations (D19) and (D20) inside Eq. (D18) we get

$$\begin{aligned} \langle \delta x^2(\theta, x, t) \rangle^c |_{\theta'} &= t d^2 \rho(\theta', x, t) |v^{\text{eff}}(\theta) - v^{\text{eff}}(\theta')| \\ &= t \rho(\theta', x, t) \mathbf{g}_{1,1}(\theta, \theta') \end{aligned} \quad (\text{D21})$$

where \mathbf{g} is the matrix defined in the main text. Integrating over the fluctuations of all quasiparticles, we get the full variance

of the quasiparticle trajectory,

$$\begin{aligned} \langle \delta x^2(\theta, x, t) \rangle^c &= t \int_{\mathbb{R}} d\theta' \rho(\theta', x, t) \mathbf{g}_{1,1}(\theta, \theta') \\ &= t \text{diag}(\mathfrak{D}_{[\rho]}^{(1,1)}), \end{aligned} \quad (\text{D22})$$

where $\text{diag}(\mathfrak{D}_{[\rho]}^{(1,1)})$ is the diagonal part of the (1, 1) component of the diffusion matrix $\mathfrak{D}_{[\rho]}$.

Now we take into consideration the variance of the trajectories in the momentum space. Using the same argument presented above, we can express it in terms of density fluctuations,

$$\begin{aligned} \langle \delta \theta^2(\theta, x, t) \rangle^c |_{\theta'} &= t^2 \langle (\delta a^{\text{eff}})^2 \rangle^c |_{\theta'} \\ &= t^2 \left(\frac{\delta a^{\text{eff}}(\theta)}{\delta n(\theta')} \right)^2 \langle \delta n(\theta')^2 \rangle^c, \end{aligned} \quad (\text{D23})$$

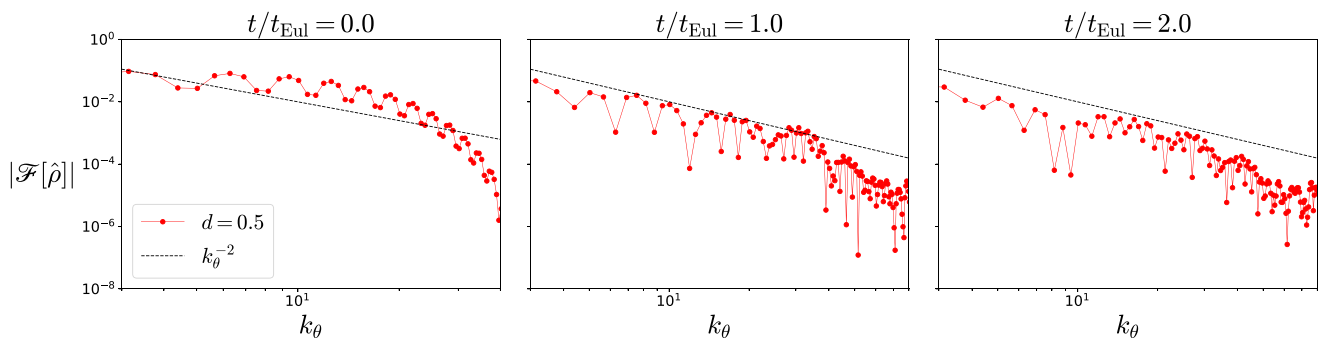


FIG. 7. Exact hard rods gas evolution with $m_0(x) = 0$ and $V_0 = 0.5$ and $\ell = 80$, initialized in a Bragg pulse state with width $T_0 = 0.01$. Log-Log plot of the absolute value of the Fourier transforms in θ of the spatially integrated density estimated through exact numerical simulations of hard rods with rods' length $d = 0.5$. The data are shown as a function of Fourier vector k_θ . The behavior of the system, in this case, is qualitatively the same as the one shown in Fig. 3 of the main text, although we can resolve a smaller range of momenta compared to GHD simulations due to Monte Carlo noise.

where the fluctuations $\langle \delta n(\theta')^2 \rangle^c$ are evaluated again over an interval of length $\Lambda = |v^{\text{eff}}(\theta) - v^{\text{eff}}(\theta')|t$. The derivative of the effective acceleration with respect to the generalized Fermi factor can be computed from Eq. (B6) as is

$$\frac{\delta a^{\text{eff}}(\theta, x, t)}{\delta n(\theta', x, t)} = d(1 - \bar{\rho}(x, t)d)(a^{\text{eff}}(\theta, x, t) - a^{\text{eff}}(\theta', x, t)). \quad (\text{D24})$$

Using the relations (D19) and (D24) in Eq. (D23) we get

$$\begin{aligned} \langle \delta \theta^2(\theta, x, t) \rangle^c |_{\theta'} &= t d^2 \rho(\theta', x, t) \frac{(a^{\text{eff}}(\theta) - a^{\text{eff}}(\theta'))^2}{|v^{\text{eff}}(\theta) - v^{\text{eff}}(\theta')|} \\ &= t \rho(\theta', x, t) \mathbf{g}_{2,2}(\theta, \theta'). \end{aligned} \quad (\text{D25})$$

Integrating the quantity computed in Eq. (D25) over all the quasiparticles' fluctuations, we get the full variance of the trajectory in momentum space

$$\begin{aligned} \langle \delta \theta^2(\theta, x, t) \rangle^c &= t \int_{\mathbb{R}} d\theta' \rho(\theta', x, t) \mathbf{g}_{2,2}(\theta, \theta') \\ &= t \text{diag}(\mathfrak{D}_{[\rho]}^{(2,2)}). \end{aligned} \quad (\text{D26})$$

Finally, we compute the transverse variance $\langle \delta x \delta \theta(\theta, x, t) \rangle^c |_{\theta'}$ expressing it in terms of density fluctuations

$$\begin{aligned} \langle \delta x \delta \theta(\theta, x, t) \rangle^c |_{\theta'} &= t^2 \langle \delta v^{\text{eff}}(\theta) \delta a^{\text{eff}}(\theta) \rangle^c |_{\theta'} \\ &= t^2 \left(\frac{\delta v^{\text{eff}}(\theta)}{\delta n(\theta')} \frac{\delta a^{\text{eff}}(\theta)}{\delta n(\theta')} \right) \langle \delta n(\theta')^2 \rangle^c. \end{aligned} \quad (\text{D27})$$

Using relations (D20), (D24), and (D19) into Eq. (D27) we get

$$\begin{aligned} \langle \delta x \delta \theta(\theta, x, t) \rangle^c |_{\theta'} &= t d^2 \rho(\theta, x, t) \text{sgn}(v^{\text{eff}}(\theta) - v^{\text{eff}}(\theta')) \\ &\quad \times (a^{\text{eff}}(\theta) - a^{\text{eff}}(\theta')) \\ &= t \rho(\theta', x, t) \mathbf{g}_{1,2}(\theta, \theta'). \end{aligned} \quad (\text{D28})$$

Integrating Eq. (D28) over all possible momenta θ' we get the full variance of the trajectory in the transverse direction

$$\begin{aligned} \langle \delta x \delta \theta(\theta, x, t) \rangle^c &= t \int_{\mathbb{R}} d\theta' \rho(\theta', x, t) \mathbf{g}_{1,2}(\theta, \theta') \\ &= t \text{diag}(\mathfrak{D}_{[\rho]}^{(1,2)}). \end{aligned} \quad (\text{D29})$$

Thus, from Eqs. (D22), (D26), and (D29), we conclude that the quasiparticles' trajectories broaden diffusively in phase space. Namely, the variance of a single particle's probability distribution in phase space grows linearly in time with a coefficient equal to the diagonal part of the diffusion matrices $\mathfrak{D}_{[\rho]}$ previously defined in Eq. (B11):

$$\begin{aligned} \langle \mathbf{R} \otimes \mathbf{R}(\theta, x, t) \rangle^c &= t \begin{pmatrix} \text{diag}(\mathfrak{D}_{[\rho]}^{(1,1)}(\theta, \theta')) & \text{diag}(\mathfrak{D}_{[\rho]}^{(1,2)}(\theta, \theta')) \\ \text{diag}(\mathfrak{D}_{[\rho]}^{(1,2)}(\theta, \theta')) & \text{diag}(\mathfrak{D}_{[\rho]}^{(2,2)}(\theta, \theta')) \end{pmatrix}. \end{aligned} \quad (\text{D30})$$

APPENDIX E: ADDITIONAL NUMERICAL DATA

In this Appendix we present the following numerical results

(1) In Fig. 6 we show the absolute value of the Fourier transform in θ of the spatially integrated density given by the GHD evolution with $m_0 = 0.5$ and $V_0 = 0$. We observe that, in the presence of a space dependent mass, the behavior of this quantity is qualitatively the same as in the presence of a potential trap, shown in Fig. 3 of the main text.

(2) In Fig. 7 we show the absolute value of the Fourier transform in θ of the spatially integrated density given by the exact hard rods gas evolution with $V_0 = 0.5$ and $m_0 = 0$. The results are qualitatively the same as in Fig. 3 of the main text. Although GHD is expected not to be predictive in the turbulent phase, it mimics the correct qualitative behavior for this quantity.

-
- [1] M. Rigol, A. Muramatsu, and M. Olshanii, Hard-core bosons on optical superlattices: Dynamics and relaxation in the superfluid and insulating regimes, *Phys. Rev. A* **74**, 053616 (2006).
- [2] M. Rigol, V. Dunjko, V. Yurovsky, and M. Olshanii, Relaxation in a completely integrable many-body quantum system: An *ab initio* study of the dynamics of the highly excited states of 1D lattice hard-core bosons, *Phys. Rev. Lett.* **98**, 050405 (2007).
- [3] M. Rigol, V. Dunjko, and M. Olshanii, Thermalization and its mechanism for generic isolated quantum systems, *Nature (London)* **452**, 854 (2008).
- [4] D. A. Abanin, E. Altman, I. Bloch, and M. Serbyn, Colloquium: Many-body localization, thermalization, and entanglement, *Rev. Mod. Phys.* **91**, 021001 (2019).
- [5] J. Eisert, M. Friesdorf, and C. Gogolin, Quantum many-body systems out of equilibrium, *Nat. Phys.* **11**, 124 (2014).
- [6] T. Kinoshita, T. Wenger, and D. S. Weiss, A quantum Newton's cradle, *Nature (London)* **440**, 900 (2006).
- [7] I. Bloch, J. Dalibard, and W. Zwerger, Many-body physics with ultracold gases, *Rev. Mod. Phys.* **80**, 885 (2008).
- [8] Y. Tang, W. Kao, K.-Y. Li, S. Seo, K. Mallayya, M. Rigol, S. Gopalakrishnan, and B. L. Lev, Thermalization near integrability in a dipolar quantum Newton's cradle, *Phys. Rev. X* **8**, 021030 (2018).
- [9] M. Schemmer, I. Bouchoule, B. Doyon, and J. Dubail, Generalized hydroDynamics on an atom chip, *Phys. Rev. Lett.* **122**, 090601 (2019).
- [10] F. Møller, C. Li, I. Mazets, H.-P. Stimming, T. Zhou, Z. Zhu, X. Chen, and J. Schmiedmayer, Extension of the generalized hydrodynamics to the dimensional crossover regime, *Phys. Rev. Lett.* **126**, 090602 (2021).
- [11] D. Wei, A. Rubio-Abadal, B. Ye, F. Machado, J. Kemp, K. Srakaew, S. Hollerith, J. Rui, S. Gopalakrishnan, N. Y. Yao, I. Bloch, and J. Zeiher, Quantum gas microscopy of Kardar-Parisi-Zhang Superdiffusion, *Science* **376**, 716 (2022).
- [12] N. Malvania, Y. Zhang, Y. Le, J. Dubail, M. Rigol, and D. S. Weiss, Generalized hydrodynamics in strongly interacting 1D Bose gases, *Science* **373**, 1129 (2021).
- [13] Y. Le, Y. Zhang, S. Gopalakrishnan, M. Rigol, and D. S. Weiss, Observation of hydrodynamization and local prethermalization in 1D Bose gases, *Nature (London)* **618**, 494 (2023).
- [14] J. M. Deutsch, Quantum statistical mechanics in a closed system, *Phys. Rev. A* **43**, 2046 (1991).

- [15] M. Srednicki, Chaos and quantum thermalization, *Phys. Rev. E* **50**, 888 (1994).
- [16] F. H. L. Essler and M. Fagotti, Quench dynamics and relaxation in isolated integrable quantum spin chains, *J. Stat. Mech.* (2016) 064002.
- [17] E. Altman, Many-body localization and quantum thermalization, *Nat. Phys.* **14**, 979 (2018).
- [18] L. Vidmar and M. Rigol, Generalized Gibbs ensemble in integrable lattice models, *J. Stat. Mech.* (2016) 064007.
- [19] H. Spohn, *Large Scale Dynamics of Interacting Particles* (Springer, Berlin, 1991).
- [20] R. L. D. C. Boldrighini and Y. M. Sukhov, One-dimensional hard rod caricature of hydrodynamics, *J. Stat. Phys.* **31**, 577 (1983).
- [21] J. K. Percus, Exact solution of kinetics of a model classical fluid, *Phys. Fluids* **12**, 1560 (1969).
- [22] B. Doyon and H. Spohn, Drude weight for the Lieb-Liniger Bose gas, *SciPost Phys.* **3**, 039 (2017).
- [23] B. Doyon and H. Spohn, Dynamics of hard rods with initial domain wall state, *J. Stat. Mech.* (2017) 073210.
- [24] B. Doyon, T. Yoshimura, and J.-S. Caux, Soliton gases and generalized hydrodynamics, *Phys. Rev. Lett.* **120**, 045301 (2018).
- [25] O. A. Castro-Alvaredo, B. Doyon, and T. Yoshimura, Emergent hydrodynamics in integrable quantum systems out of equilibrium, *Phys. Rev. X* **6**, 041065 (2016).
- [26] B. Bertini, M. Collura, J. De Nardis, and M. Fagotti, Transport in out-of-equilibrium XXZ chains: Exact profiles of charges and currents, *Phys. Rev. Lett.* **117**, 207201 (2016).
- [27] V. B. Bulchandani, R. Vasseur, C. Karrasch, and J. E. Moore, Bethe-Boltzmann hydrodynamics and spin transport in the XXZ chain, *Phys. Rev. B* **97**, 045407 (2018).
- [28] J. De Nardis, D. Bernard, and B. Doyon, Hydrodynamic diffusion in integrable systems, *Phys. Rev. Lett.* **121**, 160603 (2018).
- [29] A. Bastianello, B. Doyon, G. Watts, and T. Yoshimura, Generalized hydrodynamics of classical integrable field theory: the sinh-Gordon model, *SciPost Phys.* **4**, 045 (2018).
- [30] E. Ilievski and J. De Nardis, Ballistic transport in the one-dimensional Hubbard model: The hydrodynamic approach, *Phys. Rev. B* **96**, 081118(R) (2017).
- [31] V. B. Bulchandani, On classical integrability of the hydrodynamics of quantum integrable systems, *J. Phys. A* **50**, 435203 (2017).
- [32] M. Fava, S. Biswas, S. Gopalakrishnan, R. Vasseur, and S. A. Parameswaran, Hydrodynamic nonlinear response of interacting integrable systems, *Proc. Natl. Acad. Sci. USA* **118**, e2106945118 (2021).
- [33] B. Bertini and L. Piroli, Low-Temperature Transport in Out-of-Equilibrium XXZ Chains, *J. Stat. Mech.* (2018) 033104.
- [34] B. Pozsgay, Current operators in integrable spin chains: lessons from long-range deformations, *SciPost Phys.* **8**, 016 (2020).
- [35] A. Bastianello, V. Alba, and J.-S. Caux, Generalized hydrodynamics with space-time inhomogeneous interactions, *Phys. Rev. Lett.* **123**, 130602 (2019).
- [36] A. Bastianello, J. De Nardis, and A. De Luca, Generalized hydrodynamics with dephasing noise, *Phys. Rev. B* **102**, 161110(R) (2020).
- [37] R. Koch, A. Bastianello, and J.-S. Caux, Adiabatic formation of bound states in the one-dimensional Bose gas, *Phys. Rev. B* **103**, 165121 (2021).
- [38] A. Bastianello and A. De Luca, Integrability-protected adiabatic reversibility in quantum spin chains, *Phys. Rev. Lett.* **122**, 240606 (2019).
- [39] J. Lopez-Piqueres and R. Vasseur, Integrability breaking from backscattering, *Phys. Rev. Lett.* **130**, 247101 (2023).
- [40] S. Scopa, P. Calabrese, and L. Piroli, Generalized hydrodynamics of the repulsive spin- $\frac{1}{2}$ Fermi gas, *Phys. Rev. B* **106**, 134314 (2022).
- [41] R. Senaratne, D. Cavazos-Cavazos, S. Wang, F. He, Y.-T. Chang, A. Kafle, H. Pu, X.-W. Guan, and R. G. Hulet, Spin-charge separation in a one-dimensional Fermi gas with tunable interactions, *Science* **376**, 1305 (2022).
- [42] V. E. Zakharov, V. S. L'vov, and G. Falkovich, *Kolmogorov Spectra of Turbulence I* (Springer, Berlin, 1992).
- [43] J. L. Lebowitz, J. K. Percus, and J. Sykes, Time evolution of the total distribution function of a one-dimensional system of hard rods, *Phys. Rev.* **171**, 224 (1968).
- [44] H. Spohn, Hydrodynamical theory for equilibrium time correlation functions of hard rods, *Ann. Phys.* **141**, 353 (1982).
- [45] L. Tonks, The complete equation of state of one, two and three-dimensional gases of hard elastic spheres, *Phys. Rev.* **50**, 955 (1936).
- [46] A. Robledo and J. S. Rowlinson, The distribution of hard rods on a line of finite length, *Mol. Phys.* **58**, 711 (1986).
- [47] C. B. Mendl and H. Spohn, Equilibrium time-correlation functions for one-dimensional hard-point systems, *Phys. Rev. E* **90**, 012147 (2014).
- [48] C. Boldrighini and Y. M. Sukhov, One-dimensional hard rod caricature of hydrodynamics: Navier-Stokes correction for locally-equilibrium initial states, *Commun. Math. Phys.* **189**, 577 (1997).
- [49] J. Durnin, A. de Luca, J. de Nardis, and B. Doyon, Diffusive hydrodynamics of inhomogeneous Hamiltonians, *J. Phys. A* **54**, 494001 (2021).
- [50] S. Gopalakrishnan, D. A. Huse, V. Khemani, and R. Vasseur, Hydrodynamics of operator spreading and quasiparticle diffusion in interacting integrable systems, *Phys. Rev. B* **98**, 220303(R) (2018).
- [51] S. Gopalakrishnan and R. Vasseur, Kinetic theory of spin diffusion and superdiffusion in XXZ spin chains, *Phys. Rev. Lett.* **122**, 127202 (2019).
- [52] T. Prosen, Lower bounds on high-temperature diffusion constants from quadratically extensive almost-conserved operators, *Phys. Rev. E* **89**, 012142 (2014).
- [53] B. Doyon, Diffusion and superdiffusion from hydrodynamic projections, *J. Stat. Phys.* **186**, 25 (2022).
- [54] J.-S. Caux, B. Doyon, J. Dubail, R. Konik, and T. Yoshimura, Hydrodynamics of the interacting Bose gas in the Quantum Newton Cradle setup, *SciPost Phys.* **6**, 070 (2019).
- [55] X. Cao, V. B. Bulchandani, and J. E. Moore, Incomplete thermalization from trap-induced integrability breaking: lessons from classical hard rods, *Phys. Rev. Lett.* **120**, 164101 (2018).
- [56] A. Bastianello, A. De Luca, B. Doyon, and J. De Nardis, Thermalization of a trapped one-dimensional Bose gas via diffusion, *Phys. Rev. Lett.* **125**, 240604 (2020).
- [57] F. Møller, N. Besse, I. E. Mazets, H.-P. Stimming, and N. J. Mauser, The dissipative generalized hydrodynamic equations and their numerical solution, *J. Comput. Phys.* **493**, 112431 (2023).

- [58] Y. Bezzaz, L. Dubois, and I. Bouchoule, Rapidity distribution within the defocusing non-linear Schrödinger equation model, *SciPost Phys. Core* **6**, 064 (2023).
- [59] M. Kulkarni, G. Mandal, and T. Morita, Quantum quench and thermalization of one-dimensional fermi gas via phase-space hydrodynamics, *Phys. Rev. A* **98**, 043610 (2018).
- [60] D. Bagchi, J. Kethepalli, V. B. Bulchandani, A. Dhar, D. A. Huse, M. Kulkarni, and A. Kundu, Unusual ergodic and chaotic properties of trapped hard rods, *Phys. Rev. E* **108**, 064130 (2023).
- [61] N. Navon, A. L. Gaunt, R. P. Smith, and Z. Hadzibabic, Emergence of a turbulent cascade in a quantum gas, *Nature (London)* **539**, 72 (2016).
- [62] N. Navon, C. Eigen, J. Zhang, R. Lopes, A. L. Gaunt, K. Fujimoto, M. Tsubota, R. P. Smith, and Z. Hadzibabic, Synthetic dissipation and cascade fluxes in a turbulent quantum gas, *Science* **366**, 382 (2019).
- [63] M. Galka, P. Christodoulou, M. Gazo, A. Karailiev, N. Dogra, J. Schmitt, and Z. Hadzibabic, Emergence of isotropy and dynamic scaling in 2D wave turbulence in a homogeneous bose gas, *Phys. Rev. Lett.* **129**, 190402 (2022).
- [64] M. Gallone, M. Marian, A. Ponomorov, and S. Ruffo, Burgers turbulence in the Fermi-Pasta-Ulam-Tsingou chain, *Phys. Rev. Lett.* **129**, 114101 (2022).
- [65] R. Koch, J.-S. Caux, and A. Bastianello, Generalized hydrodynamics of the attractive non-linear Schrödinger equation, *J. Phys. A* **55**, 134001 (2022).
- [66] G. D. V. D. Vecchio, A. Bastianello, A. D. Luca, and G. Mussardo, Exact out-of-equilibrium steady states in the semi-classical limit of the interacting Bose gas, *SciPost Phys.* **9**, 002 (2020).
- [67] M. Mestyán and V. Alba, Molecular dynamics simulation of entanglement spreading in generalized hydrodynamics, *SciPost Phys.* **8**, 055 (2020).
- [68] B. Doyon, Lecture notes on generalised hydrodynamics, *SciPost Phys. Lect. Notes* **18** (2020).
- [69] J. D. Nardis, D. Bernard, and B. Doyon, Diffusion in generalized hydrodynamics and quasiparticle scattering, *SciPost Phys.* **6**, 049 (2019).
- [70] P. Fendley and H. Saleur, Nonequilibrium dc noise in a luttinger liquid with an impurity, *Phys. Rev. B* **54**, 10845 (1996).